Highlights

- Microfibrillated cellulose (MFC) films loaded with lysozyme were prepared.
- MFC's nano-sized dimensions enabled slowing the release of lysozyme over time.
- The release of lysozyme was higher for simulant A than simulant C.
- The release did not change significantly at 6°C and 23°C.
- MFC can be used as a 'release suppressor' agent in controlled release systems.

Graphical Abstract

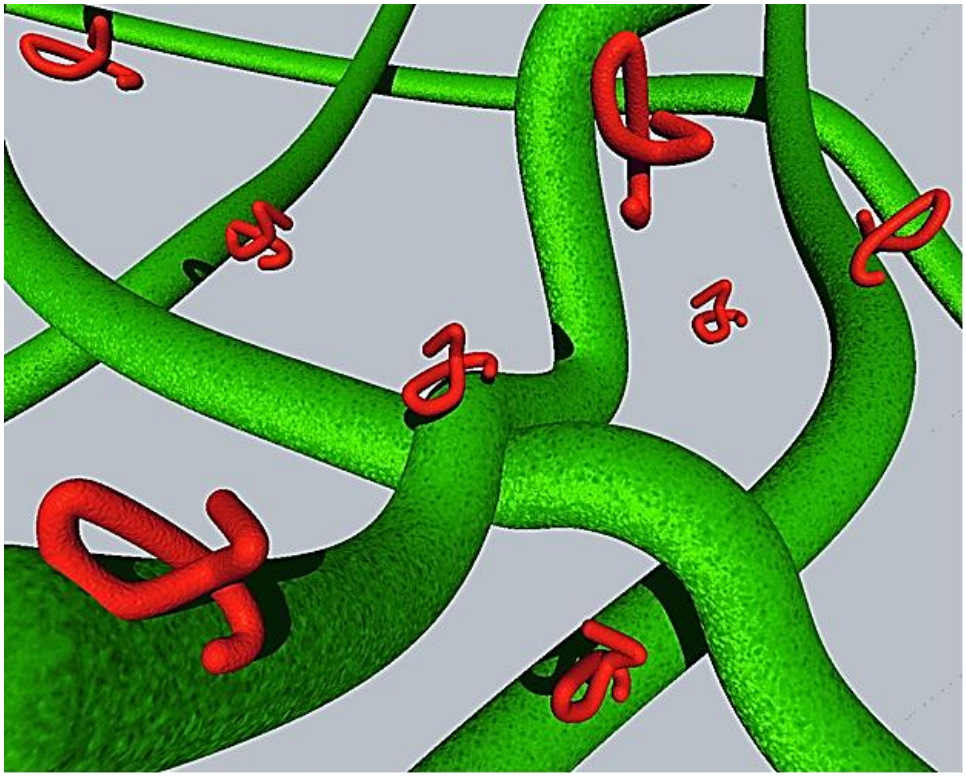

Schematic representation of the active films given by the antimicrobial molecule lysozyme entrapped within the microfibrillated cellulose network

Exploiting the nano-sized features of microfibrillated cellulose (MFC) for the development of controlled-release packaging

Carlo A. Cozzolino[a,b], Fritjof Nilsson[c], Marco Iotti[b], Benedetta Sacchi[d], Antonio Piga[a], Stefano Farris[e]*

[a]*STAA, Department of Agriculture—University of Sassari, Viale Italia 39/A, 07100 Sassari, Italy*

[b]*PFI, Norwegian Pulp and Paper Research Institute—Høgskoleringen 6b, NO-7491 Trondheim, Norway*

[c]*Department of Fiber and Polymer Technology, KTH Royal Institute of Technology, SE-10044, Stockholm, Sweden*

[d]*Interdepartmental Center of Advanced Microscopy, CIMA, University of Milan Via Celoria 26—20133 Milan, Italy*

[e]*DeFENS, Department of Food, Environmental and Nutritional Sciences, Packaging Division—University of Milan, Via Celoria 2—20133 Milan, Italy*

---

*__Corresponding author__: S. Farris; Tel.: +39 0250316654; Fax: +39 0250316672

Email address: stefano.farris@unimi.it

Abstract

Microfibrillated cellulose (MFC) was used in this study to prepare films containing an active molecule, lysozyme, which is a natural antimicrobial agent. The main goal of this research was to assess the potential for exploiting the nano-sized dimension of cellulose fibrils to slow the release of the antimicrobial molecule, thus avoiding a too-quick release into the surrounding medium, which is a major disadvantage of most release systems. For this purpose, the release kinetics of lysozyme over a 10-day period in two different media (pure water and water/ethanol 10 wt.%) were obtained, and the experimental data was fitted with a solution of Fick's second law to quantify the apparent diffusion coefficient (*D*). The results indicate that the MFC retained lysozyme, presumably due to electrostatic, hydrogen, and ion-dipole interactions, with the largest release of lysozyme—approximately 14%—occurring from the initial amount loaded on the films. As expected, ethanol as a co-solvent slightly decreased the diffusion of lysozyme from the MFC polymer network. The addition of two potential modulating release agents—glycerol and sodium chloride—was also evaluated. Findings from this work suggest that MFC-based films can be considered a suitable candidate for use in controlled-release packaging systems.

Keywords: controlled release; diffusion; modeling; nano-sized; microfibrillated cellulose; lysozyme

1. Introduction

Cellulose is one of the most important polysaccharides and abundant biopolymers on earth [1]. It consists of a linear β-glucose homopolymer with subunits called cellobiose, β-1,4 linked glucose [2]. The cellulose chains are arranged in strands of cellulose microfibrils [3] immersed in a matrix of hemicellulose and lignin. The literature uses several terms to describe MFC: microfibrils [**4**], microfibril aggregates [5], microfibrillar cellulose [6], nanofibrils [7], nanofibers [8], nanofibrillar cellulose [9], and fibril aggregates [10]. According to the conventional nomenclature, in which "nano" refers to particles between 0.001 and 0.1 microns (1 to 100 nm), MFC can be defined as nano-fibrils with diameters of less than 100 nm, lengths of several micrometers [11,12], and an aspect ratio (length/diameter, L/d) between 100 and 150 [13]. MFC are composed of amorphous and crystalline regions [11] that, together with both large specific surface area and reactive –OH groups [12], contribute to its excellent mechanical properties, such as stiffness and tensile strength [14], that have been exploited for various purposes [7]. Applications of MFC include, but are not limited to, reinforcement in nanocomposite materials [15,16], dispersion stabilizers [17], filtration media [18], and oxygen barrier material in food and pharmaceutical products [6]. However, very little research dealing with the development of active materials based on MFC and designed for antimicrobial applications has been conducted [19,20].

The past decade, though, has witnessed a rapid increase in research into the development of active films intended for food packaging applications, particularly alternative methods for controlling both microbial contamination and detrimental oxidation in foods in order to limit, inhibit, or delay the growth of microorganisms and the rate of quality decay [21–23]. Among other bioactive compounds, lysozyme has received great attention in recent years as a natural

biopreservative for antimicrobial packaging applications [24,25]. Lysozyme (Figure 1), classified as a food additive by European Directive 95/2/EC, is an ellipsoidal, globular protein stabilized by disulfide bonds that has a molecular mass of 14 kDa, an isoelectric point of pH 11.1, and a net charge of +9 per molecule at a pH of 5.6 [26]. Lysozyme can be found in many human secretions (tears, saliva, mucus), as well as in egg whites. Its antimicrobial activity has been attributed to the hydrolysis of the β-1,4 linkage between *N*-acetyl muramic acid and *N*-acetyl glucosamine present in peptidoglycan. That is why lysozyme is more effective against Gram-positive bacteria (whose cell wall is composed of 90% peptidoglycan) than against Gram-negative bacteria (where peptidoglycan accounts for only 5–10%) [24,27]. Lysozyme-containing active packaging has successfully been used for ready-to-eat thin-cut veal meat [28], cold-smoked salmon [29,30], ground beef patties [31], ready-to-eat turkey bologna [32], pork loins [33], and minced meat [34], just to provide some examples. However, evidence from literature on lysozyme-based active packaging systems has shown that the antimicrobial effect is limited to a short time, mainly due to a too-rapid delivery from the polymer network. For example, Gemili et al. showed that a 100% release of lysozyme from films made of cellulose acetate in contact with distilled water at 4°C occurred between 40 minutes and 7 hours, depending on the amount of cellulose acetate used to prepare the films [35]. Park et al., working on chitosan-lysozyme composite films, found that the percentage of lysozyme released from the films after 48 hours in a 0.15 M phosphate buffer (pH 6.2) at 25°C ranged between 65% and 76% as a function of the initial amount of the antimicrobial molecule included in the polymer matrix [36]. Hiwale et al. demonstrated that, irrespective of the fabrication method adopted, a 100% release of lysozyme from cross-linked gelatin microspheres in a phosphate buffer (pH 7.4) at 37°C took place after approximately 6 days [37].

It has previously been demonstrated that achieving the controlled release of active molecules over time is the key to extending the shelf life of perishable foods [38]. Controlled-release packaging (CRP), which allows for the slow and modulated release of active compounds from packaging into food, has been proven more effective than adding active compounds directly into food [39] when shelf life extension is the target. Among other methods to create an effective CRP system, such as modification of the packaging's polymer structure or encapsulation of the active compounds, the physicochemical interactions between the polymer matrix and loaded molecules may dictate the ultimate release attributes of the packaging system [40].

The goal of this study was to assess the potential of cellulose fibrils as a "release suppressor" (which prevents a too-quick release of the active molecule into the surrounding medium) for the generation of new bionanocomposites with antimicrobial properties, by exploiting: i) the electrostatic forces [20,41] between MFC (which carries an overall negative charge) and the enzyme lysozyme (which carries an overall positive charge for pHs below its isoelectric point); ii) the nano-dimensional structure of the cellulose polymer network, which might help retain the active molecule within the polymer matrix because of the interface effect (i.e., more polymer-active molecule interactions than occur in macro-sized networks such as paper, paperboard, and plastics). This property could enable switching, according to the classification proposed by Han [42], from an unconstrained, free diffusion mode to a slow diffusion mode or, possibly, a reservoir system, in which the release of the active molecule can be assumed to remain constant for a longer time span, thus extending the shelf life of foods. These modes are schematically shown in Figure 2. Accordingly, the release kinetics of lysozyme from MFC films were investigated in this work over an extended temporal window of 10 days, by estimating a quantifiable parameter (the diffusion coefficient) as a function of two food

simulants (simulant A–water and simulant C–water/ethanol 10 wt.%) at two temperatures (6°C and 23°C). The release kinetics of the active compound were also estimated in the presence of two release-modulating agents, glycerol and sodium chloride. To the best of our knowledge, this is the first work dealing with the potential use of MFC as a "release-suppressing" agent for the development of controlled-release systems.

2. Materials and methods

2.1. Materials

MFC was produced at the Paper and Fibre Research Institute (PFI, Trondheim, Norway) using two different types of cellulose—(1) Elemental chlorine-free (ECF), fully-bleached sulphate pulp mainly based on juvenile *Picea abies*, and (2) ECF, fully-bleached sulphate cellulose mainly based on mature *Picea abies* with up to 5 wt.% pine (*Pinus sylvestris*)—following the manufacturing procedure described by Turbak and Herrik [43,44]. The main physicochemical characteristics of the manufactured MFC have been described in previous papers [6,45]. Lysozyme from chicken egg-white powder (crystalline, approximately 70,000 units/mg) was purchased from Sigma-Aldrich (Oslo, Norway). Glycerol (redistilled, min 99.5% $^{w}/_{v}$) was purchased from VWR International (Leuven, Belgium). Sodium chloride was purchased from Merck (Darmstadt, Germany). Milli-Q water with a resistivity higher than 18.2 MΩ cm and ethanol (Fluka Analytical, Oslo, Norway) were used for the preparation of the hydro-alcoholic solutions (water/ethanol 10 wt.%).

2.2. Films preparation

Three different batches of films were prepared for the release tests: 1) MFC films including lysozyme (10 wt.% = 1g/10g MFC), coded as M-L10; 2) M-L10, also including glycerol (4 wt.% = 0.4g/10g MFC), coded as M-L10-G4; and 3) M-L10, also including NaCl (10 wt.% = 1g/10g MFC), coded as M-L10-N10. For all three batches, an initial 0.89 wt.% water dispersion of MFC was used as the starting MFC reservoir. Before incorporation into the MFC matrix, the lysozyme powder was dissolved in cold water at room temperature for 2 hours under gentle stirring (100 rpm). The third component (glycerol and NaCl for samples M-L10-G4 and M-L10-N10, respectively) was added as the final step in the preparation of the MFC-lysozyme water dispersion, which was then left to settle for 2 hours. At this point, a known amount of the MFC antimicrobial water dispersion was poured into Petri dishes (∅ 8.5 cm). This procedure was selected to ensure consistency between the theoretical active compound loaded in the MFC matrix and the actual amount entrapped in the final films. The resulting samples were then stored for three days at 23°C and 65% RH. At this point, films were peeled off from the plastic substrate and cut in 5×2 cm^2 strips, which were in turn stored in a climatic chamber (23°C and 50% RH) for 1 week. The thickness of each sample was measured at 10 random positions with a digital micrometer (Micrometer 51 Lorentzen & Wettre, Stockholm, Sweden).

2.3. Lysozyme release kinetics

Lysozyme-loaded MFC films were put into flasks containing two different contact media (50 mL)—distilled water and water/ethanol 10 wt.% solution—which are designated as food simulants (simulant A and simulant C, respectively) in the food contact material legislation [46]. The lysozyme release experiments were conducted over 10 days (after which the release from the

MFC films was no longer observed) by keeping the flasks at 6°C and 20°C under moderate shaking (100 rpm) using a Flask Dancer 270292 orbital shaker from Boekel Scientific (Feasterville, PA, USA). The choice for this temperatures accounts for the most common storage conditions of packaged food; i.e., refrigerated and temperate (room temperature) conditions. Although of potential relevance to assessment of the stability of the enzymatic system, a wider temperature range was not considered due to the already-reported thermal stability of lysozyme. Indeed, it has been extensively reported that the activity of lysozyme is fully preserved up to at least 75°C, which makes lysozyme also suitable for incorporation into biopolymer matrices during extrusion [47–49]. Interestingly, it has been demonstrated that the lytic activity of lysozyme is retained up to 90°C when the protein below its isoelectric point is combined with anionic polyelectrolytes (e.g., cellulose) [24]. The release kinetics of lysozyme were determined by measuring the lysozyme concentration in the simulant at different intervals by recording the absorption at 280 nm [34] using a Lambda 650 UV/VIS spectrophotometer (PerkinElmer, Waltham, MA, USA). The absorbance values were then converted into concentration values using the calibration curve, which was calculated as the means of standard solutions (three replicates) from 50 ppm to 250 ppm (mg/kg). Each data point on the release curves represents the mean of nine replicates.

2.4. Conductometric titration

The charge density of MFC was determined by conductometric titration following the method described in a previous study [50]. Briefly, a MFC aqueous dispersion (0.1 wt.%) was treated with an excess (15 mL) of 0.1 N hydrochloric acid (HCl) to completely neutralize the negative charge potentially distributed along the cellulose backbone. Conductometric titration

was performed by adding 0.1 N sodium hydroxide (NaOH) under gentle stirring (100 rpm). Ionic conductivity was evaluated after sequential injections of 0.1 mL drops of NaOH at 0.40 μL s^{-1}. As the conductance decreased and the first equivalence point was approached, drops of 0.05 mL at a 0.15 μL s^{-1} flow rate were dispensed, while the initial set-up conditions were brought back beyond the constant-conductivity region. The titrant was added approximately every 60 s to allow for sufficient time to reach equilibrium between readings, while the pH was measured continuously. Finally, the charge density (mmol g^{-1}) was quantified by a graphical method, plotting the measured ionic conductivity versus total titrant and calculating the volume (mL) of titrant required to fully deprotonate all charged groups on cellulose from the intersection points of the linear segments of the ionic conductivity plot before and after the equivalent point (or breakpoint).

2.5. Electron microscopy analyses

Cross-sections and surfaces of MFC films were examined with a Leo 1430 scanning electron microscopy (Zeiss, Oberkochen, Germany) to gather data on the overall physical organization of the polymer network. Surface test specimens were mounted with carbon tape on stubs. Cross-sectioned samples were cut into thin pieces with a scalpel and mounted on a thin specimen split-mount holder to examine the cross-section. Before being inserted into the microscope, the samples were sputter coated with gold to a thickness of approximately 10 nm using an Agar High Resolution Sputter Coater (model 208RH) equipped with a gold target/Agar thickness monitor controller.

Transmission electron microscopy (TEM) images were captured to visualize the MFC fibrils dimension. To this end, 5 μL of a 0.1 wt.% MFC aqueous uranyl acetate water dispersion

were placed on a Formvar-coated Cu grid (400 mesh). Observations were made after 24 hours (the time required to allow the solvent to evaporate) using an LEO 912 AB energy-filtering transmission electron microscope (EFTEM) (Carl Zeiss, Oberkochen, Germany) operating at 80 kV. Digital images were recorded with a ProScan 1K Slow-Scan CCD camera (Proscan, Scheuring, Germany).

2.6. Laser profilometry analysis

Laser profilometry tests were also conducted to check for any potential influence of lysozyme, glycerol, and NaCl on the surface morphology of the MFC films. Samples of approximately 1×1 cm^2 were mounted on an object glass with double-sided tape. The samples were covered with a layer of gold before image acquisition. Images were acquired from 10 areas of each film. The topography images were 1×1 mm^2, with a resolution of 1 μm/pixel. The analysis was performed with the SurfCharJ plug-in. Lateral structures larger than 40 μm were suppressed.

2.7. Statistical analysis

The statistical significance of differences in the release and surface roughness of films was determined by one-way analysis of variance (ANOVA), using JMP 5.0.1 software (SAS, Cary, NC, USA). Where appropriate, the mean values were compared through a Student's t-test with a significance level of (p) < 0.05. The lysozyme kinetic release curves were determined by fitting the analytical solution of Fick's second law for a planar sheet to the experimental data solved using Matlab® (The Mathworks Inc., Natick, MA, USA).

3. Results and discussion

3.1. Lysozyme release kinetics

The overall release process of low molecular-weight compounds (such as lysozyme) from strongly hydrophylic networks (such as MFC) can be the result of three phenomena: 1) solvent diffusion into the film network, 2) relaxation of the polymer matrix due to the swelling of the strongly hydrophilic MFC molecules, and 3) diffusion of the active compound from the swollen polymeric network into the surrounding medium. The experimental release data were modeled assuming that: 1) both water diffusion and relaxation of molecular chains occur faster than the diffusion of the low molecular-weight antimicrobial compound through the swollen network; 2) lysozyme diffusion takes place in an homogeneous, symmetric medium; 3) the volume of the liquid medium is infinite; and 4) the external mass transfer coefficient at the solid-liquid interface is negligible. In addition, modeling was performed only on experimental data from the first diffusion part of the release curve for all samples, which was the time between the start of the experiments (t = 0) and the appearance of the first steady state level. Any secondary diffusion process associated with a sudden jump in the release curve was not considered.

The solution of Fick's second law for a planar sheet with constant boundary conditions, thus, can be used [51]:

$$M_t = M_\infty \left\{ 1 - \frac{8}{\pi^2} \sum_{n=0}^{n=\infty} \frac{1}{(2n+1)^2} \exp\left[-\frac{D_{LYS}}{l^2} (2n+1)^2 \pi^2 t \right] \right\}, \qquad (1)$$

where M_t represents the amount (mg/kg) of the diffusing compound released at time t (s); M_∞ is the corresponding amount at infinite time (e.g., at equilibrium), taken as the initial quantity loaded on the film; D_{LYS} is the lysozyme apparent diffusion coefficient ($cm^2\ s^{-1}$) through the MFC polymer matrix; and l is the thickness (cm) of dry films. The release kinetics were obtained by

plotting the M_t / M_∞ ratio versus the square root of time in order to evaluate the diffusion behavior of the low molecular-weight antimicrobial molecule according to the classification proposed by Crank [51].

Figures 3 and 4 display the experimental and simulated release data for the three film types under different conditions (simulant A and C at 6°C and 23°C). As an overall consideration, the total amount of lysozyme released in the medium never reached values as high as 100% over the time considered in this research. Therefore, the main goal of the study was satisfactorily achieved, because the quick release of all the antimicrobial initially loaded on the polymer films was avoided. Significantly, the MFC network's ability to retain lysozyme was pronounced, insomuch as approximately 13% of the lysozyme was released after 10 days in the experiment. This finding can be explained by first considering the newly-established weak interactions between MFC and lysozyme. In particular, MFC carries a net negative charge because of the carboxylic acid groups in the hemicellulose fraction and oxidation residues produced by refining the raw material of the main cellulose skeleton [52]. As confirmed by our conductometric measurements (see Figure 5), the negative charge was 0.7925 ± 0.01 mmol g^{-1}, which is far lower than other negative polyelectrolyte biopolymers such as pectin [50]. Therefore, it is plausible that moderate electrostatic interactions took place between the negatively-charged MFC and positively-charged lysozyme. However, ion-dipole interactions between lysozyme and the polar pendant hydroxyl groups of cellulose also could have contributed to limiting the diffusion of lysozyme through the MFC network [40].

The density of the aforementioned MFC/lysozyme interactions is an equally important factor in determining the final release performance of the MFC matrix. This physical aspect is intimately linked to MFC's nano-sized features. As shown in Figure 6a, MFC is composed of

fibrils 3 to 100 nm wide and approximately 10 μm long, which is in agreement with previous observations [53]. In contrast, wood fibers have been shown to typically be 1 to 3 mm long and roughly 10 to 50 μm wide (Figure 6b). The higher aspect ratio (the length-to-diameter ratio) of MFC fibrils compared to wood fibers ultimately results in a better ability to interact with other molecules, such as lysozyme, because of the higher number of binding sites per unit volume. This consideration is in line with what was already observed; i.e., the density of ionic interactions between MFC and lysozyme increases with decreasing size of the cellulosic fibers [24].

3.2. Influence of the type of simulant

For the same polymer system at the same temperature, the total lysozyme released was always higher for simulant A than for simulant C (compare Figure 3a with Figure 3c, and Figure 4a with Figure 4c). This finding likely reflects the hydrophilic nature of the antimicrobial molecule—namely, its higher affinity for water than ethanol. At the same time, while water is a strong solvent for the polymer matrix, ethanol has only partial affinity with MFC and, thus, triggers the release of the active compound to a lesser extent. However, this observation (higher release values for the simulant A) is not supported by the estimation of the apparent diffusion coefficients, as shown in Table 1. As a tentative explanation, the overall release kinetics of lysozyme from the hydro-alcoholic solution are governed exclusively by the diffusion of the active molecule across the polymer network to the medium; conversely, it can be clearly seen that, when only water is used as a simulant, diffusion is predominant in the initial rise in each curve, but after a certain time, secondary effects occurred, indicated by the sudden jumps in the release of lysozyme (see arrows in Figure 3a). As already reported [40], the appearance of the

film burst in hydrophilic polymers can reasonably be attributed to the partial collapse of the semi-crystalline regions, which certainly occurs after the dissolution of the amorphous phase. The final result was an increase in the lysozyme released into the surrounding medium (water).

3.3. Influence of temperature

With the exception of the glycerol-containing samples, there was no statistical difference in the release patterns of the samples stored at 6°C and 23°C; therefore, the increase in temperature cannot be considered a trigger in the release of lysozyme from the MFC-based films, at least within the thermal range tested in this experiment. Most likely, this finding is due to MFC's low sensitivity to temperature changes. Indeed, like most cellulosic materials, MFC's thermal properties, which are intimately linked to its highly cohesive nature (with a glass transition temperature higher than its degradation temperature), mainly caused by extensive hydrogen bonding, allow the polymer matrix to almost entirely preserve its physical arrangement even after a change from 6°C to 23°C [54,55]. This finding has practical relevance: the release of lysozyme in MFC-based packaging will not be affected by different storage conditions, such as temperatures commonly used in the food supply chain.

The *D* reduction with increasing T for samples plasticized with glycerol is still somehow unclear. A tentative explanation could be the enhanced mobility of glycerol at 23°C, which eventually prompted new interactions between the active molecule and glycerol, thus constraining the free motion of lysozyme across the polymer matrix. However, further investigation may clarify the effect of glycerol on the availability of lysozyme in the MFC release system.

3.4. Influence of glycerol and NaCl

As demonstrated in the values of the apparent diffusion coefficients for the M-L10 and M-L10-G4 samples (Table 1), glycerol, as expected, triggered the release of the active molecule in the water medium (simulant A) at both temperatures (6°C and 23°C) due to its well-known plasticizing effect [56]. Newly-established interactions between glycerol molecules and the main polysaccharide backbone have also been suggested as possible causes [56]. Eventually, this competition between glycerol and lysozyme to bind the main MFC chains should have favored the release of the antimicrobial molecule into the water medium. Conversely, glycerol thwarted the release of lysozyme from the MFC matrix when exposed to the hydro-alcoholic medium (simulant C). As reported in a similar study, it is likely that water-ethanol-glycerol interactions modify the availability of water molecules for the polymer matrix, thus slowing the relaxation of the polymer chains [40].

The addition of NaCl apparently hindered the release of lysozyme. This effect can be attributed to changes in the MFC's molecular arrangement caused by the presence of the salt. More specifically, while the electrostatic repulsion between negatively charged groups prevents fibril-fibril interactions in a low-concentration regime, aggregation is prompted as the ionic strength increases (the screening effect) [57]. This effect, in turn, is reflected in a more constrained structure, which was confirmed by the cross-section SEM images of the three different MFC-based samples (Figure 7). Accordingly, the difference in thickness between the NaCl-loaded samples (M-L10-N10) and the other two samples (M-L10 and M-L10-G4) was statistically significant, because the M-L10-N10 sample shrunk and had a lower thickness because of the salt-induced aggregation of fibrils (Table 1).

3.5. Surface morphology of the MFC-based films

The final morphology of a film (both of plastic and natural origin) is an important parameter, because it can dramatically affect interfacial phenomena such as wettability, light scattering, and ease of contamination [58,59]. This effect is reflected in some final properties of the films, such as the optical properties, and in the various finishing operations, including deposition of protective coatings, printing, and lamination, to which the films can be subjected after fabrication. An overall view of the surface topography of the three MFC-based samples is provided in Figure 8. As shown in Table 1, although there was not a remarkable difference among the samples, the glycerol-loaded sample (M-L10-G4) had the smoothest surface, while there was no statistically-significant difference between the M-L10 and M-L10-N10 films. The addition of glycerol likely reduced the intra-molecular aggregation of cellulose fibrils, leading to an overall relaxation of the MFC network and, hence, a less bumpy surface. The highest surface roughness measured on the M-L10-N10 films can be attributed to the surfacing of some salt crystals, as clearly shown in Figure 7c.

4. Conclusions

This study approached the still-open issue of CRP systems from a nanotechnology perspective. Our goal was to demonstrate that the release of a small-molecule active compound can be controlled by exploiting the nano-sized characteristics of the polymer network. This research successfully demonstrated that the MFC films are a suitable carrier for the antimicrobial lysozyme, preventing its fast release during the early stages of contact with the two food simulants tested (water and water/ethanol solutions). The observed performance, which was attributed to an interface effect, yielded over-retention of the active molecule in the final films.

The MFC release systems were also insensitive to changes in temperature (6°C and 23°C). Additionally, the use of two modulating agents showed that, to some extent, the release can be fine-tuned by acting on the physicochemical properties (e.g., the aggregation state of the fibrils) of the main MFC network.

Findings from this work suggest that MFC can be profitably used as a minor component in the formulation of release devices to slow the release of active molecules from the main polymer network. Potential applications include, but are not limited to, food packaging, where lysozyme-based antimicrobial systems have been suggested (e.g., for fresh fish, fresh meat, and minimally-processed vegetables).

Acknowledgements

We are thankful to Dr. Gary Chinga-Carrasco for the laser profilometry analysis, and Marianne Lenes (PFI) and Størker Moe (NTNU) for valuable discussions.

References

[1] I. Siró, D. Plackett, Cellulose, 17 (2010) 459.

[2] A. Cabiaca, E. Guillon, F. Chambon, C. Pinel, F. Rataboul and N. Essayem, Appl. Catal. A-Gen., 402 (2011) 1.

[3] L. Berglund, New Concepts in Natural Fibres Composites, 27th Risø International Symposium on Material Science, Risø National Laboratory, Roskilde, Denmark, 2006.

[4] C. Aulin, I. Varga, P.M. Claesson, L. Wågberg and T. Lindström, Langmuir, 24 (2008) 2509.

[5] S. Iwamoto, A.N. Nakagaito and H. Yano, Appl. Phys. A., 89 (2007) 461.

[6] K. Syverud, P. Stenius, Cellulose**,** 16 (2009) 75.

[7] S. Ahola, J. Salmi, L.S. Johansson, J. Laine and M. Österberg, Biomacromolecules, 9 (2008) 1273.

[8] K. Abe, S. Iwamoto and H. Yano, Biomacromolecules, 8 (2007) 3276.

[9] M. Pääkkö, J. Vapaavuori, R. Silvennoinen, H. Kosonen, M. Ankerfors, T. Lindström, L.A. Berglund and O. Ikkala, Soft Matter, 4 (2008) 2492.

[10] T. Virtanen, S.L. Maunu, T. Tamminen, B. Hortling and T. Liitiä, Carbohyd. Polym., 73 (2008) 156.

[11] G. Chinga-Carrasco, Nanoscale Res. Lett., 6 (2011) 417.

[12] K. Syverud, G. Chinga-Carrasco, J. Toledo and P.G. Toledo, Carbohydr. Polym., 84 (2011) 1033.

[13] M.A. Hubbe, O.J. Rojas, L.A. Lucia and M. Sain, Bio Res., 3 (2008) 929.

[14] J. Lu, T. Wang and L.T. Drzal, Compos. Part A-Appl. S., 39 (2008) 738.

[15] A. López-Rubio, J.M. Lagaron, M. Ankerfors, T. Lindström, D. Nordqvist, A. Mattozzi and M.S. Hedenqvist, Carbohydr. Polym., 68 (2007) 718.

[16] Y. Srithep, L.S. Turng, R. Sabo and C. Clemons, Cellulose, 19 (2012) 1209.

[17] M. Andresen, P. Stenius, J. Dispers. Sci. Technol., 28 (2007) 837.

[18] C. Burger, B.S. Hsiao and B. Chu, Annu. Rev. Mater. Res., 36 (2006) 333.

[19] M. Andresen, P. Stenstad, T. Møretrø, S. Langsrud, K. Syverud, L.S. Johansson and P. Stenius, Biomacromolecules, 8 (2007) 2149.

[20] N.C.T. Martins, C.S.R. Freire, R.J.B. Pinto, S.C.M. Fernandes, C.P. Neto, A.J.D. Silvestre, J. Causio, G. Baldi, P. Sadocco and T. Trindade, Cellulose, 19 (2012) 1425.

[21] R.D. Joerger, Packag. Technol. Sci., 20 (2007) 231.

[22] S. Quintavalla, L. Vicini, Meat Sci., 62 (2002) 373.

[23] A. Rodríguez, R. Batlle and C. Nerín, Prog. Org. Coat., 60 (2007) 33.

[24] E. Mascheroni, G. Capretti, M. Marengo, S. Iametti, L. Mora, L. Piergiovanni and F. Bonomi, Packag. Technol. Sci., 23 (2010) 47.

[25] H.R. Ibrahim, S. Higashiguchi, M. Koketsu, L.R. Juneja, M. Kim, T. Yamamoto, Y. Sugimoto and T. Aoki, J. Agric. Food Chem., 44 (1996) 3799.

[26] H.M. Gorr, J.M. Zueger, D.R. McAdams, and J.A. Barnard, Colloids Surf. B, 103 (2013) 59.

[27] J.N. Losso, S. Nakai, S., E.A. Charter, in A. S. Naidu (Ed.), Natural food antimicrobial systems, CRC Press LLC, Boca Raton, 2000, pp. 185–210.

[28] A. Barbiroli, F. Bonomi, G. Capretti, S. Iametti, M. Manzoni, L. Piergiovanni, M. Rollini, Food Control, 26 (2012) 387.

[29] S. Min, L.J. Harris, J.H. Han, J.M. Krochta, J. Food Prot., 68 (2005), 2317.

[30] S. Min, T.R. Rumsey, J.M. Krochta, J. Food Eng. 84 (2008) 39.

[31] I. Uysal Unalan, F. Korel, A. Yemenicioglu, Int. J. Food Sci. Technol. 46 (2011) 1289.

[32] S. Mangalassary, I. Han, J. Rieck, J. Acton, P. Dawson, Food Microbiol. 25 (2008) 866.

[33] F.M. Nattress, L.P. Baker, Int. J. Food Microbiol. 85 (2003) 259.

[34] M.S. Rao, R. Chander, A. Sharma, LWT - Food Sci. Technol. 41 (2008) 1995.

[35] S. Gemili, A. Yemenicioğlu and S.A. Altınkay, J. Food Eng., 90 (2009) 453.

[36] S.-I. Park, M.A. Daeschel andY. Zhao, J. Food Sci., 69 (2004) M215.

[37] P. Hiwale, S. Lampis, G. Conti, C. Caddeo, S. Murgia, A.M. Fadda, M. Monduzzi, Biomacromolecules, 12 (2011)3186.

[38] X. Chen, D.S. Lee, X. Zhu and K.L. Yam, J. Agric. Food Chem., 60 (2012) 3492.

[39] X. Zhu, K.M. Schaich, X. Chen, D. Chung and K.L. Yam, Food Res. Int., 47 (2012) 1.

[40] C.A. Cozzolino, T.O.J. Blomfeldt, F. Nilsson, A. Piga, L. Piergiovanni and S. Farris, Colloid. Surface. A, 403 (2012) 45.

[41] S.L. Turgeon, C. Schmitt and C. Sanchez, Curr. Opin. Colloid In. 12 (2007) 166.

[42] J.H. Han, in J.H. Han (Ed.), Innovations in Food Packaging, 1st Edition, Elsevier, San Diego, 2005, Chapter 6.

[43] A.F. Turbak, F.W. Snyder and K.R. Sandberg, J. Appl. Polym. Sci.: Appl. Polym. Symp., 37 (1983) 815.

[44] F.W. Herrick, R.L. Casebier, J.K. Hamilton and K.R. Sandberg, J. Appl. Polym. Sci.: Appl. Polym. Symp., 37 (1983) 797.

[45] M. Iotti, Ø.W. Gregersen, S. Moe and M. Lenes, J. Polym. Environ., 19 (2011) 137.

[46] Commission Regulation (EU) No 10/2011 of 14 January 2011 on Plastic Materials and Articles Intended to Come into contact with Food, Official Journal of the European Union, L 12/1 L 12/89.

[47] M. Ciolkowski, B. Pałecz, D. Appelhans, B. Voit, B. Klajnert, M. Bryszewska, Colloids Surf. B, 95 (2012) 103.

[48] T. Yamamoto, N. Fukui, A. Hori, Y. Matsui, J. Mol. Struct., 782 (2006) 60.

[49] M.A. Del Nobile, A. Conte, G.G. Buonocore, A.L. Incoronato, A. Massaro, O. Panza, J. Food Eng., 93 (2009) 1.

[50] S. Farris, L. Mora, G. Capretti and L. Piergiovanni, J. Chem. Educ., 89 (2012) 121.

[51] J. Crank, The Mathematics of Diffusion, Clarendon Press, Oxford, 1975.

[52] U. Freudenberg, R. Zimmermann, K. Schmidt, S.H. Behrens and C. Werner, J. Colloid. Interf. Sci., 309 (2007) 360.

[53] G. Chinga-Carrasco, A. Miettinen, C.L. LuengoHendriks, E.K. Gamstedt and M. Kataja, in J. Cuppoletti (Ed.), Nanocomposites and Polymers with Analytical Methods, InTech, Rijeka, Croatia, 2011, 243–260.

[54] N. Lavoine, I. Desloges, A. Dufresne and J. Bras, Carbohyd. Polym., 90 (2012) 735.

[55] R.J. Moon, A. Martini, J. Nairn, J. Simonsen and J. Youngblood, Chem. Soc. Rev., 40 (2011) 3941.

[56] E. Trovatti, S.C.M. Fernandes, L. Rubatat, D. da Silva Perez, C.S.R. Freire, A.J.D. Silvestre and C.P. Neto, Compos. Sci. Technol., 72 (2012) 1556.

[57] A.B. Fall, S.B. Lindström, O. Sundman, L. Ödberg and L. Wågberg, Langmuir 27 (2011) 11332.

[58] S. Farris, L. Introzzi, P. Biagioni, T. Holz, A. Schiraldi and L. Piergiovanni, Langmuir, 27 (2011) 7563.

[59] L. Introzzi, J.M. Fuentes-Alventosa, C.A. Cozzolino, S. Trabattoni, S. Tavazzi, C.L. Bianchi, A. Schiraldi, L. Piergiovanni and S. Farris, ACS Appl. Mater. Interfaces, 4 (2012) 3692.

Figure Captions

Figure 1. Structure of egg white lysozyme with the four disulfide bonds and the nature (hydrophilic, hydrophobic, basic, or acidic) of the amino acids sequence (adapted from reference 33).

Figure 2. Schematic representation of (a) the unconstrained, free diffusion, (b) slow diffusion, and (c) reservoir system modes of a small-molecule active compound (red spheres) in a biopolymer matrix (adapted from reference 40). Note the different structural organizations of the biopolymer network that controls the transfer of the active molecule at the biointerface.

Figure 3. Experimental (a and c) and calculated (b and d) release data of lysozyme from the M-L10 (─□─), M-L10-G4, (─○─), and M-L10-N10 (─△─) samples after 10 days (a and c) and 6 hours (b and d) of immersion at 6°C in simulant A (a and b) and in simulant C (c and d). Error bars represent the standard deviation around the mean value (n = 9).

Figure 4. Experimental (a and c) and calculated (b and d) release data of lysozyme from the M-L10 (─□─), M-L10-G4, (─○─), and M-L10-N10 (─△─) samples after 10 days (a and c) and 6 hours (b and d) of immersion at 23°C in simulant A (a and b) and simulant C (c and d). Error bars represent the standard deviation around the mean value (n = 9).

Figure 5. Mean conductometric and potentiometric titration curves for a 0.1 wt.% MFC aqueous dispersion.

Figure 6. TEM image of MFC fibrils (a) and SEM image of raw cellulosic fibers (b).

Figure 7. Cross-section SEM images of the (a) M-L10, (b) M-L10-G4, and (c) M-L10-N10 samples. Note in (c) the surfacing of some NaCl crystals on both sides of the MFC film.

Figure 8. (Left) Laser profilometry height and (right) 3D images of the a) M-L10, (b) M-L10-G4, and (c) M-L10-N10 samples.

Figure 1

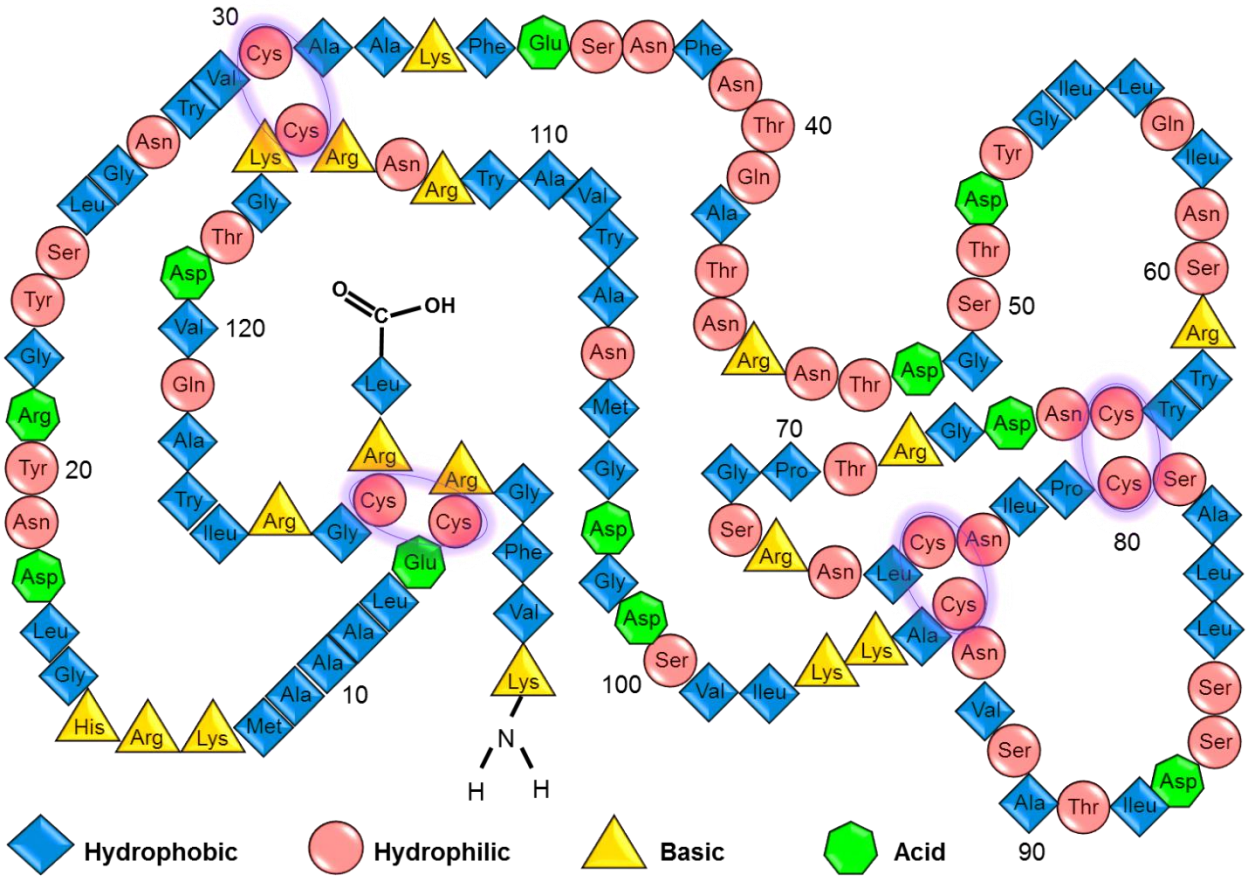

Figure 2

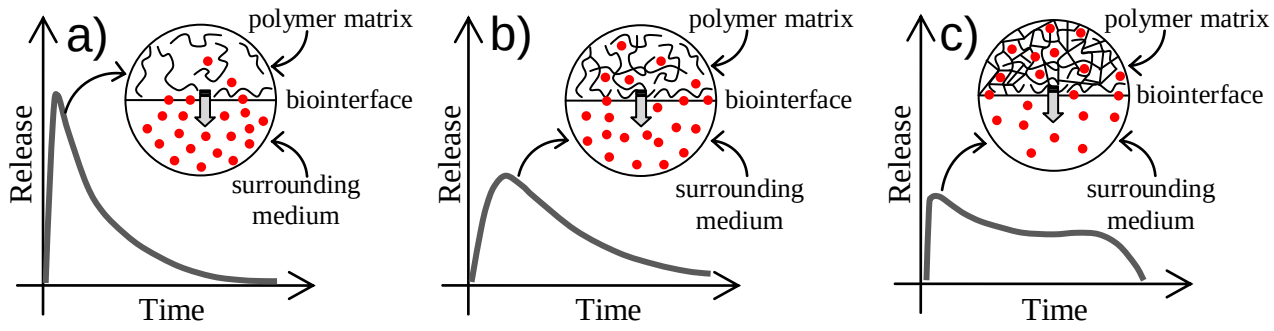
a)
polymer matrix
biointerface
surrounding medium
Release
Time
b)
polymer matrix
biointerface
surrounding medium
Release
Time
c)
polymer matrix
biointerface
surrounding medium
Release
Time

Figure 3

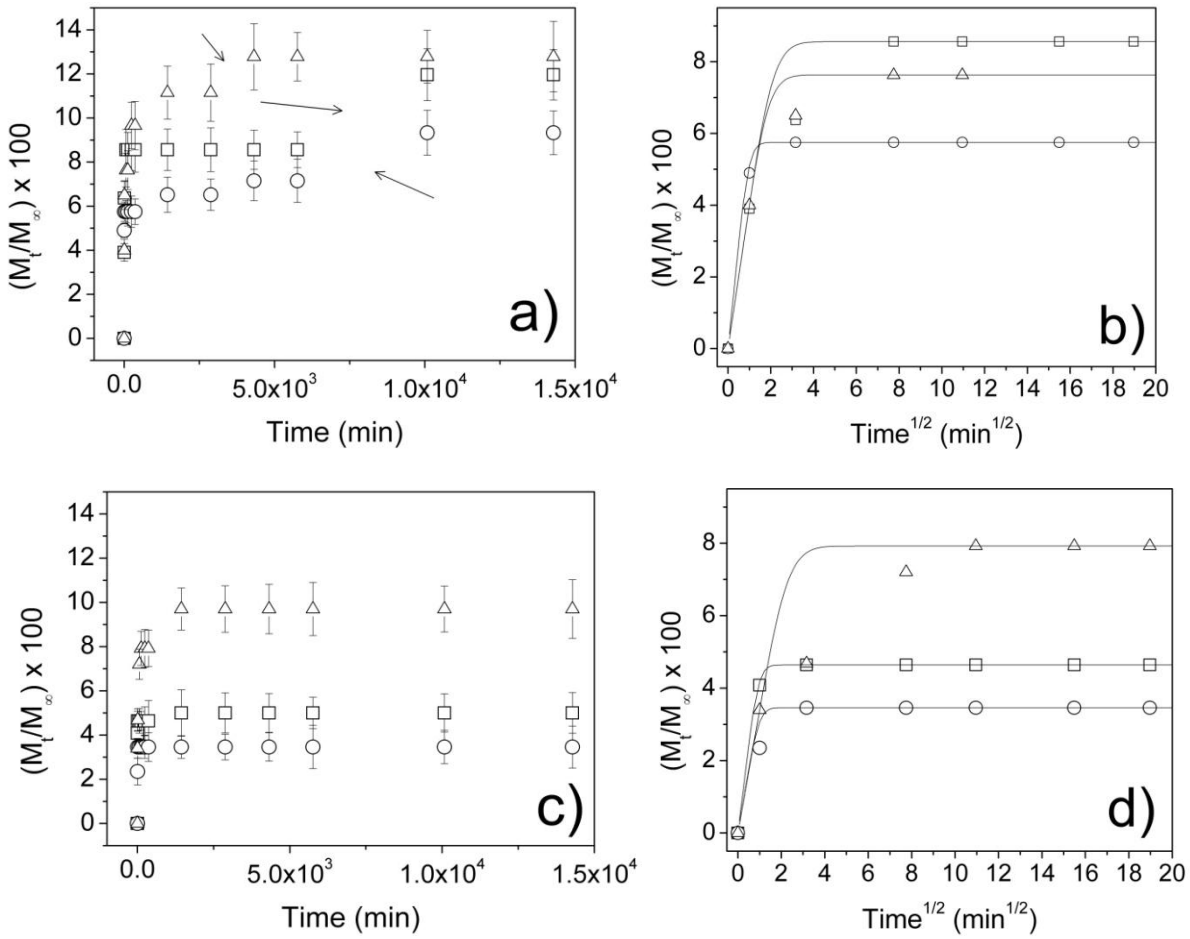
a)
b)
c)
d)
$(M_t/M_\infty) \times 100$
Time (min)
$Time^{1/2}$ ($min^{1/2}$)
0.0
$5.0x10^3$
$1.0x10^4$
$1.5x10^4$

Figure 4

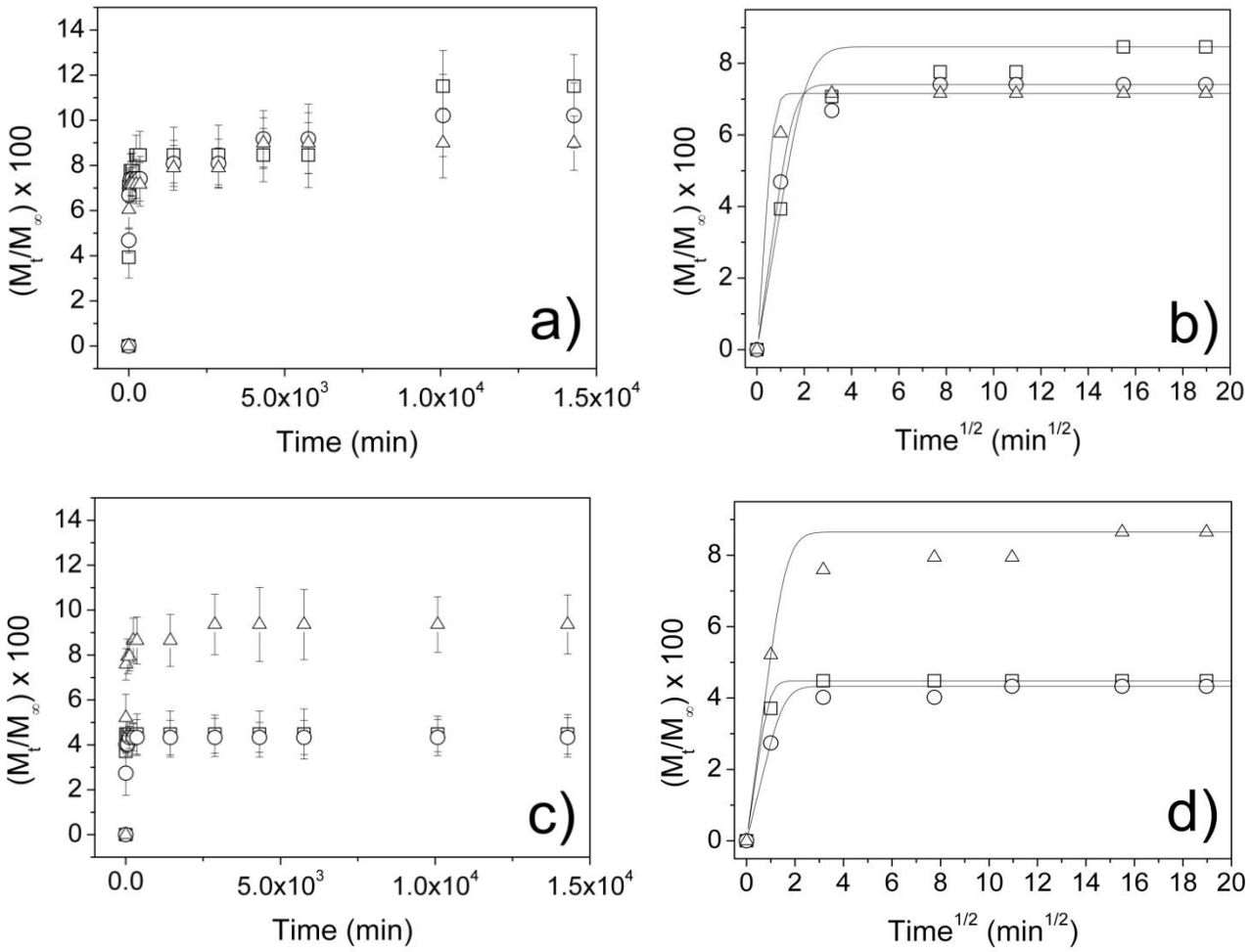
a)
b)
c)
d)
$(M_t/M_\infty) \times 100$
Time (min)
$Time^{1/2}$ $(min^{1/2})$
0.0
$5.0x10^3$
$1.0x10^4$
$1.5x10^4$

Figure 5

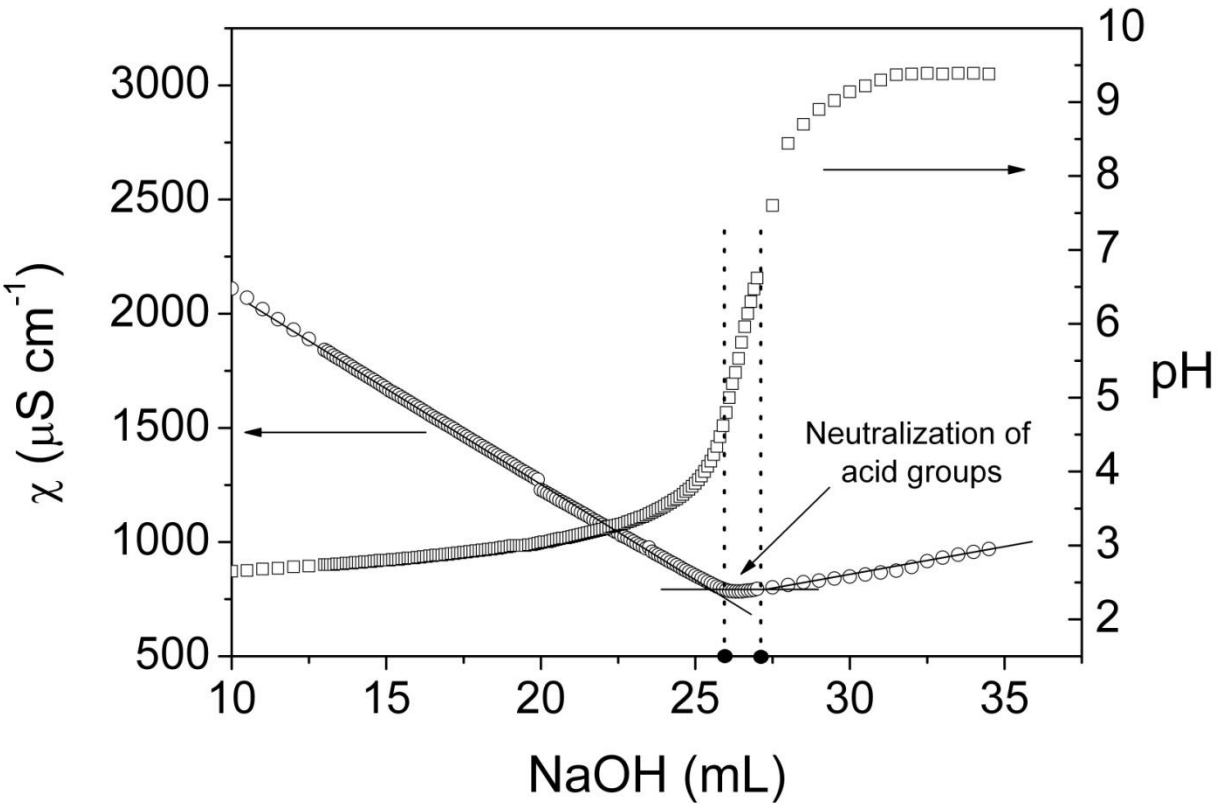
χ (μS cm-1)
pH
NaOH (mL)
Neutralization of
acid groups
3000
2500
2000
1500
1000
500
10
15
20
25
30
35
10
9
8
7
6
5
4
3
2

Figure 6

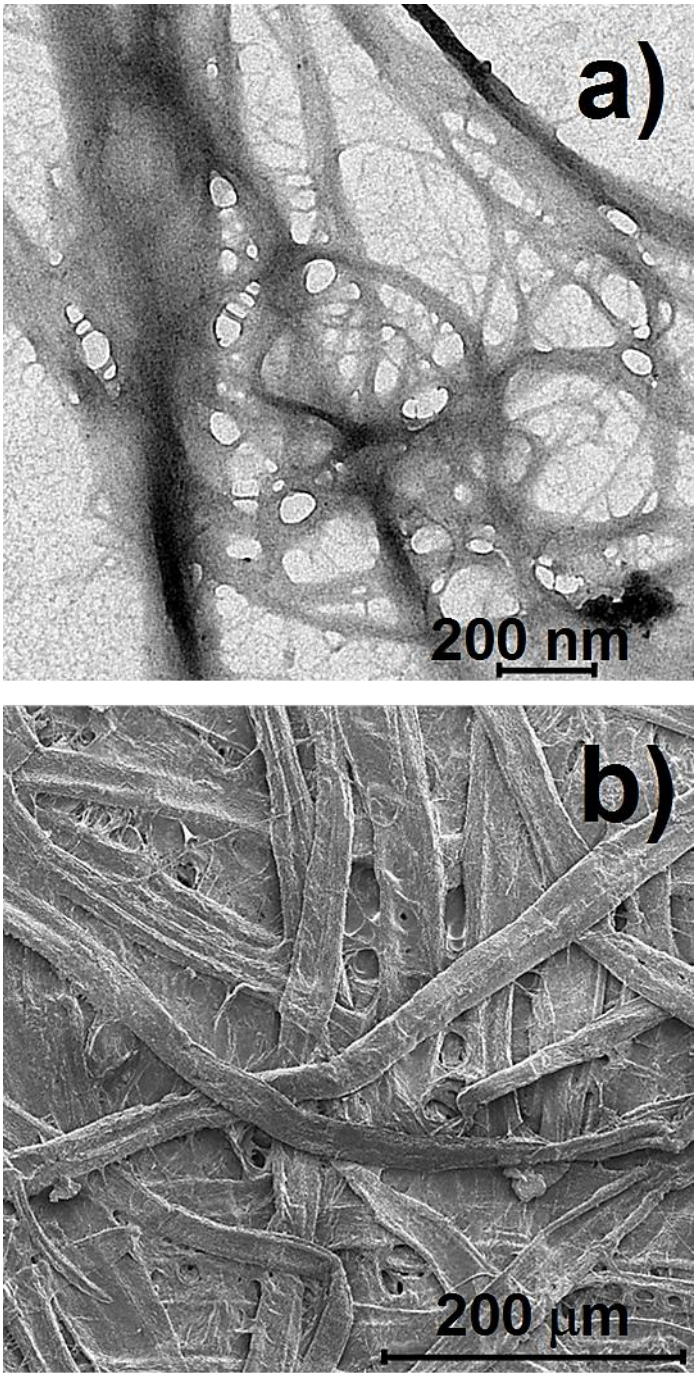

Figure 7

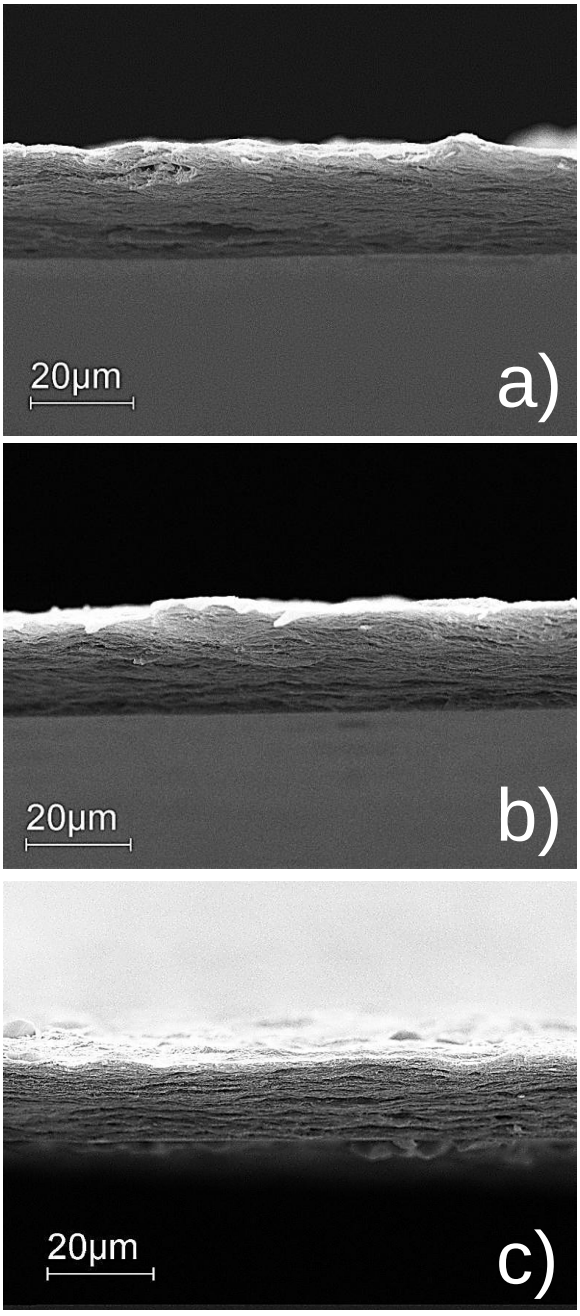

Figure 8

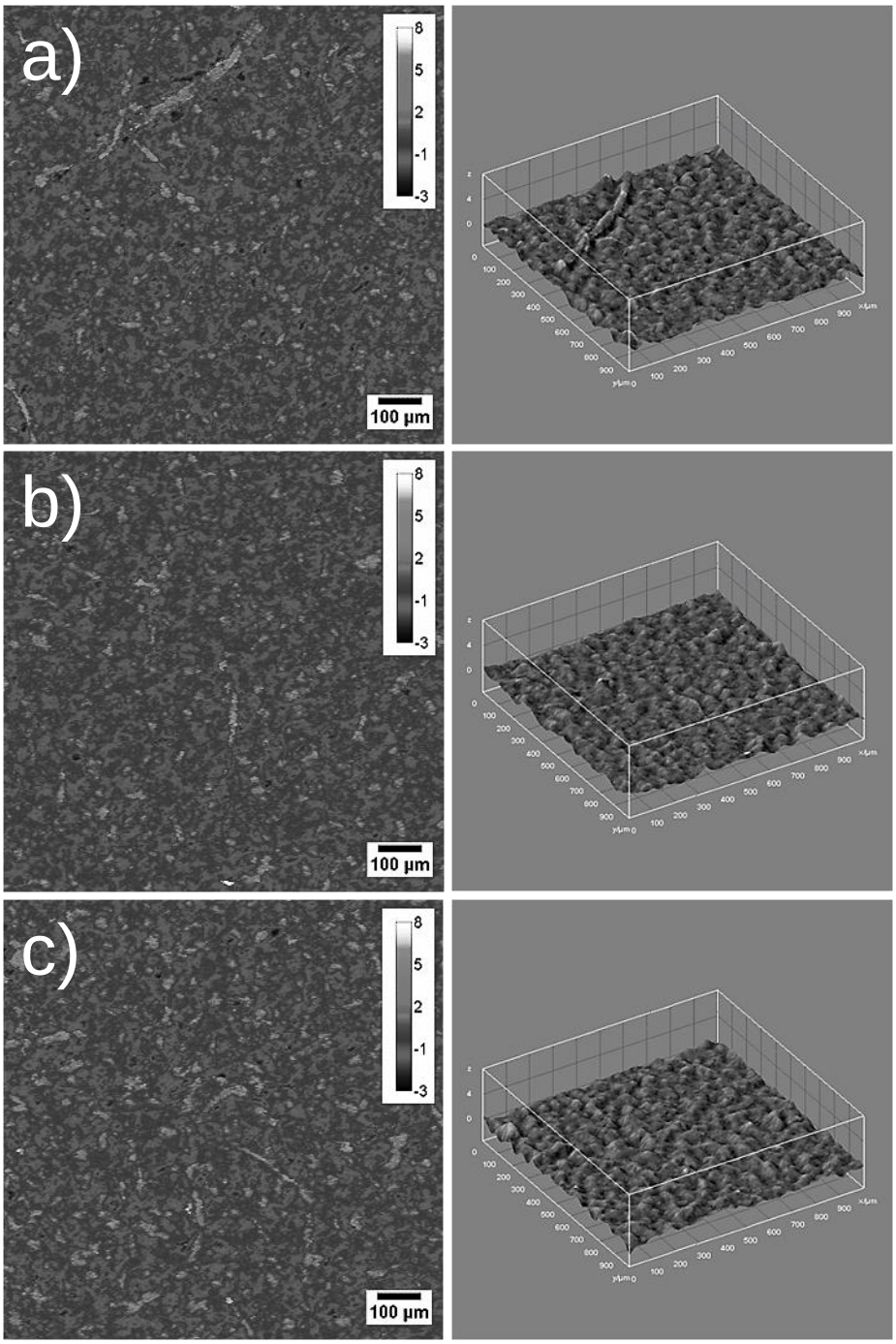

Table 1

Table 1. Thickness (*l*), diffusion coefficient (*D*), and surface roughness (*Sq*) of the MFC-based films

Film type	*l* (μm)	*D* (cm^2 s^{-1})				*Sq* (μm)
		6°C		23°C		
		Simulant A	Simulant C	Simulant A	Simulant C	
M-L10	21.67^{a} ± 1.15	$2.2E\text{-}11^{c}$	$1.2E\text{-}10^{d}$	$2.1E\text{-}11^{c}$	$1.3E\text{-}10^{d}$	0.867^{h} ± 0.040
M-L10-G4	22.33^{a} ± 0.58	$1.0E\text{-}10^{d}$	$1.0E\text{-}10^{d}$	$4.0E\text{-}11^{g}$	$4.0E\text{-}11^{g}$	0.815^{i} ± 0.031
M-L10-N10	16.67^{b} ± 0.68	$1.5E\text{-}11^{e}$	$1.0E\text{-}11^{f}$	$1.2E\text{-}10^{d}$	$2.0E\text{-}11^{c}$	0.885^{h} ± 0.024

Different superscripts within a group (i.e. within each parameter) denote a statistically significant difference ($p < 0.05$).